

## Development of Adsorbents-based Cellulose Acetate Mixed Matrix Membranes for Removal of Pollutants from Textile Industry Effluent

R. Saranya<sup>a</sup>, Y. Lukka Thuyavan<sup>b</sup>, G. Arthanareeswaran<sup>a\*</sup>

<sup>a</sup>Membrane Research Laboratory, Department of Chemical Engineering, National Institute of Technology, Tiruchirappalli-620015, India

<sup>b</sup>Division of Cell and Molecular Biology, Imperial College London, SW7 2AZ, United Kingdom

\*Corresponding author: arthanaree10@yahoo.com

### Article history

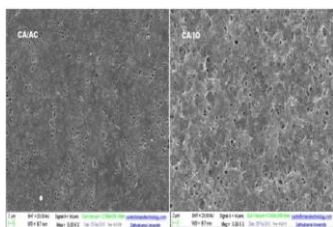
Received :1 November 2013

Received in revised form :

1 June 2014

Accepted :30 June 2014

### Graphical abstract



### Abstract

The influence of adsorbents like activated carbon (AC) and iron oxide nanoparticles (IO) on the filtration efficiency of polymeric ultrafiltration (UF) membranes is proposed to investigate by incorporating them in wt % of 0.25, 1.5 and 2.5 with cellulose acetate (CA). The completely homogenous CA/AC and CA/IO casting solutions were obtained by sonicating AC and IO, respectively in N, N'-dimethyl formamide (DMF) followed by mechanical stirring with CA. By dry/wet phase inversion technique, novel CA mixed matrix membranes (MMMs) were synthesized which were later evaluated for their characteristics using atomic force microscope (AFM), field emission scanning electron microscope (FESEM) and X-ray diffractometer (XRD). In comparison to the neat CA membrane, pure water flux of CA MMMs containing 2.5 wt % AC and 0.5 wt % IP were increased from 5.61 Lm<sup>-2</sup>h<sup>-1</sup> to 11.22 and 7.17 Lm<sup>-2</sup>h<sup>-1</sup>, respectively. These results suggest that the higher addition of AC influenced the membrane permeability whereas the amount of IP is found not to be surpassed beyond 0.5 wt% for improved flux. The wettability found by contact angle analysis suggests the higher productivity of CA MMMs and are evident by the adsorption nature of the chosen fillers. The polymer enhanced UF studies for rejecting COD, BOD and dissolved salts from the textile industry effluent has also been performed. The significance of CA MMMs lies on higher rejection efficiency with no compromise in membrane permeability.

**Keywords:** Activated carbon; iron nanoparticles; cellulose acetate; mixed matrix membranes; heavy metals

© 2014 Penerbit UTM Press. All rights reserved.

### 1.0 INTRODUCTION

Polymeric modification using reactive nanoparticles is gaining prime importance in order to enhance the filtration properties of membranes. Membranes can remove various pollutants through the separation mechanisms of impaction, diffusion, electrostatic interaction, hydrophobic property, and adsorption [1]. Among several mechanisms, adsorption is the process most commonly used in industry to remove the dye constituents of textile industry effluent. The combination of different methods like adsorption and filtration for enhanced membrane separation is highly presumed to achieve significant reduction on pollutants due to textile industries. For a long time, application of activated carbon (AC) as dye adsorbent in textile and dye wastewater treatment has been studied [2-5] because of its large surface area, polymodal porous structure, high adsorption capacity and variable surface chemical composition [6]. However, the addition of AC in organic polymer matrix for the synthesis of mixed matrix membranes (MMMs) has been very rarely studied. Ballinas *et al.* studied the influence of characters of AC on polysulfone (PSf) composite membranes in a continuous

operation system [7] and concluded the high performance of a hybrid AC/PSf composite membrane better than non-hybrid ones. The effect of polyethersulfone concentration and AC loading on the performance of MMMs in terms of permeability and selectivity of O<sub>2</sub>/N<sub>2</sub> gas separation has also been investigated [8]. Yet, the studies on application of AC coupled with membrane separation in wastewater treatment have only very less evidences.

Nanoparticles, having unique physico-chemical properties that differ from bulk materials, are of high interest in the manufacturing of membranes to achieve a high degree of control over membrane fouling and the ability to produce desired structures as well as functionalities. Nanoscale iron oxide (IO) particles due to the high surface reactivity as a result of their small size range of 1–100 nm [9] can transform chemical pollutants, such as PCBs, TCE, pesticides and chlorinated organic solvents in biosolids. It has the ability to degrade pollutants effectively by reductive [11, 12] and/or oxidative pathways depending on the state of iron [13, 14]. Several methods to synthesize IO nanoparticles were available but the main challenges of these numerous and novel techniques lie in

their capacity to obtain a narrow dispersion in particle size together with the desired compositional, structural and crystalline uniformity [15]. There are various stabilisers to obtain smaller and segregated IO nanoparticles has been studied in which the membrane [16, 17] based utilisation of IO is gaining importance in environmental remediation. The green synthesis of IO nanoparticles with the help of stabilising and reducing polyphenols is widely under research especially with the use of green tea extract. For such magnetite nanoparticles synthesis with controlled uniform particle size distribution, optimised method has to be found for high and controlled yield. The recent development of functionalized membrane makes it an ideal platform for immobilization of such reactive nanoparticles for the removal of pollutants.

The interface between a polymer matrix and inorganic filler plays an important role in the performance of MMMs. Hence, in this study, the feasibility of synthesis of AC and IO based MMMs was examined. To fully exploit the use of AC and IO for an adsorbent enhanced membrane filtration, different wt % of AC and IO was solution blended with cellulose acetate (CA). The source for IO nanoparticles was identified as the reduction reaction between green tea extract and ferric chloride. The influence of adsorption and reaction of incorporated nanoparticles owing to dispersion was confirmed by ultrasonication followed by which the CA/AC and CA/IO membranes have been successfully synthesized by phase inversion method. The characteristics of MMMs in terms of surface morphology, particle size distribution have been studied by field emission scanning electron microscopy (FESEM), x-ray diffraction (XRD) respectively. The performance of prepared MMMs was also evaluated for its permeability and rejection efficiency of chemical oxygen demand (COD), biological oxygen demand (BOD) and sulphates from textile dye effluent by means of polymer enhanced ultrafiltration.

## 2.0 EXPERIMENTAL

### 2.1 Materials

All chemicals and reagents used were of analytical grade and used without any further purification. Cellulose acetate (CA) was obtained from Sigma Aldrich, India limited. N, N'-dimethyl formamide (DMF) was purchased from Qualigens fine chemicals, Glaxo India limited. Ferric chloride was procured from Merck India Limited. Double distilled and Millipore water were produced in the laboratory.

### 2.2 Green Synthesis of Iron Oxide Nanoparticles

The synthesis of iron oxide nanoparticles with polyphenols as the reducing agent has been illustrated in many research works [18]. In this study, the reaction of ferric chloride with green tea extract forms the basis for the preparation of iron particles. 0.5 M ferric chloride and brewed green tea leaves extract was mixed in the ratio of 2:1 and kept under stirring at 250 rpm in ambient conditions. Later, the solution was centrifuged for 10 min at 6000 rpm by which the pellet remained has been washed twice with deionised water.

### 2.3 Preparation of CA/IO and CA/AC Mixed Matrix Membranes

The phase inversion method of membrane synthesis was followed for fabrication of CA/IO and CA/AC mixed matrix membranes. Different CA dope solutions were prepared by

dissolving distinct composition of IO and AC with CA. The composition of casting solution is provided in detail in Table.1. The homogenous casting solution for each composition was obtained by dissolving IO and AC initially in DMF solvent which after complete dissolution by means of ultrasonication was mixed with CA under mechanical stirring. The final doped solution was also sonicated for 30 min before casting to ensure homogeneity and casted on a cleaned glass plate. The thickness of the membrane was fixed as 400  $\mu\text{m}$  using a film applicator (elicometer). After leaving for 30 s evaporation time, the membrane was immersed in distilled water maintained at 20°C.

**Table 1** Casting composition of synthesized MMMs

Membrane Type	Casting solution Composition			Membrane description
	CA (g)	Adsorbents (g)	DMF Solvent (ml)	
CA	4.375	-	21.7	Neat CA
CA/AC1	4.353	0.022	21.7	CA+ 0.5 wt% AC
CA/AC2	4.310	0.065	21.7	CA+ 1.5 wt% AC
CA/AC3	4.266	0.109	21.7	CA+ 2.5 wt% AC
CA/IO1	4.354	0.022	21.7	CA+ 0.5 wt% IO
CA/IO2	4.310	0.065	21.7	CA+ 1.5 wt% IO
CA/IO3	4.266	0.109	21.7	CA+ 2.5 wt% IO

### 2.4 X-ray Diffraction Studies

The X-ray diffraction (XRD) pattern has been observed for pristine as well as CA/IO and CA/AC MMMs using X-ray diffractometer (Rigaku Corporation, Japan) constituting Ni-filtered Cu K $\alpha$  as a monochromatic radiation source (40 kV, 30 mA) with scintillation counter (NaI) as a detector. The samples were run between 10° and 80° of two theta angle. The intensity peaks at various two theta angles were identified to compare the grain size (D) of the crystalline particles present in each membrane with the help of full width half maximum (FWHM) of each peak and the following Scherrer's equation.

$$D = \frac{0.9\lambda}{\beta \cos\theta} \quad (1)$$

where  $\lambda$  represents the wavelength of the X-ray.

### 2.5 Morphological Studies

The top and cross-section morphology of synthesized membranes were visualized with the help of field emission scanning electron microscopy (FESEM, Hitachi, S-4160, Japan) operated at an accelerating voltage of 20 kV. The dried membrane samples were pre-treated using Au sputtering to impart electrical conductivity. The pore structure and diameter owing to the addition of adsorbents in each MMM can be analysed. The elemental analysis of adsorbents filled membrane surface and back scattered electron dispersion was performed by energy dispersive X-ray analysis (EDAX).

### 2.6 Ultrafiltration Studies

The flat sheet mixed matrix membranes were tested using a stirred cell dead-end ultrafiltration (UF) unit (Model Cell-XFUF076, Millipore, USA). The effective area of the membranes was 38.5 cm<sup>2</sup>. The membrane compaction at 0.413 MPa was performed for 1 h prior to flux studies. Later, the test run has been started with ultrapure deionised water and the

permeate volume was collected for every 10 min followed by flux ( $J_w$ ) determination using the following Equation (2).

$$J_w = \frac{V}{A \times \Delta t} \quad (2)$$

where V, A and  $\Delta t$  are the permeate volume, membrane effective area and permeation time respectively.

## 2.7 Effluent Treatment Studies

Textile dye effluent has been employed for UF using the adsorbents filled membranes to evaluate the reduction of COD, BOD and dissolved salts. The UF experiment was carried out using the same dead-end stirred cell mentioned above and the permeate volume was collected for each 10 min. The effluent flux has been determined and the average volume. To improve the solute rejection efficiency, the effluent was dissolved in water soluble polymer PEI of 1 wt % overnight. The permeate volume was analysed for COD, BOD and sulphates using the standard methods. Then, the rejection efficiency in rejecting COD, BOD and sulphates were determined separately using the following Equation (3).

$$\% \text{ Rejection (R)} = \frac{C_f - C_p}{C_f} \quad (3)$$

where  $C_f$  and  $C_p$  are the concentration of feed and permeate respectively for COD, BOD and sulphates rejection.

## 3.0 RESULTS AND DISCUSSION

### 3.1 Morphology of IO Nanoparticles

The synthesized IO nanoparticles appeared to be spherical with clustered aggregates in black color. The aggregation is attributed due to the van der Waals forces and magnetic interactions among the particles [18]. The morphology of IO nanoparticles is shown in Figure 1(a) and the spectral measurements were recorded that indicated the elemental composition of 43.86% Fe and 57.14% of O as shown in Figure 1(b).

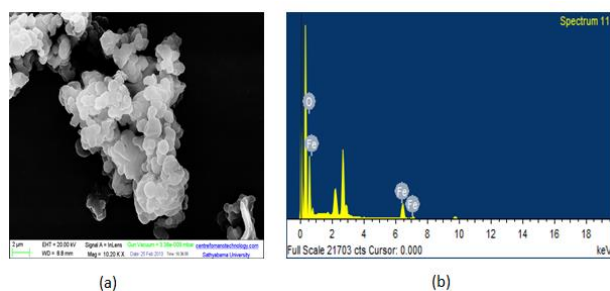


**Figure 1** SEM image (a) and EDAX spectra (b) of synthesized IO nanoparticles

### 3.2 Characterization of Synthesized MMMs

XRD pattern of the virgin CA and CA/IO MMMs of different wt% of IO nanoparticles is shown in Figure 2. The crystallite size as measured using Equation (1) indicated that the magnetite phases of Fe is characterized by 110 and 300 miller indices

which are attributed to the intensity of 30.24 and 43.38 respectively in all Fe<sub>2</sub>O<sub>3</sub> containing CA MMMs. Also, the size of the crystal was observed to increase from 4.9 nm of CA to 10.6 nm for CA/IO3 MMMs. This confirms the presence of Fe<sub>2</sub>O<sub>3</sub> nanoparticles and its crystalline behavior as the results were in agreement with the earlier reported data (Magnetite:01–111).

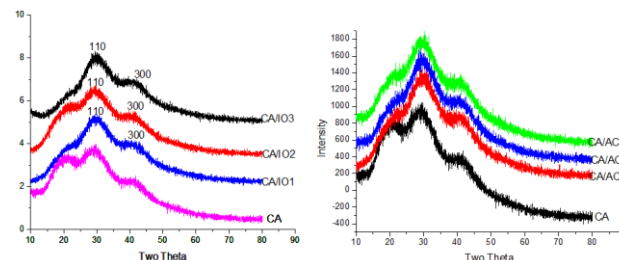


**Figure 2** XRD profile of CA/IO MMMs and CA/AC MMMs

The top surface morphology of CA/AC and CA/IO MMMs (Figure 3 A1, B1) reveals that the sonication has its significance on dispersing the nanoparticles in uniform manner in the CA matrix. The efficient dispersion of adsorbents would provide more accessible active sites for pollutants to be adsorbed [19].

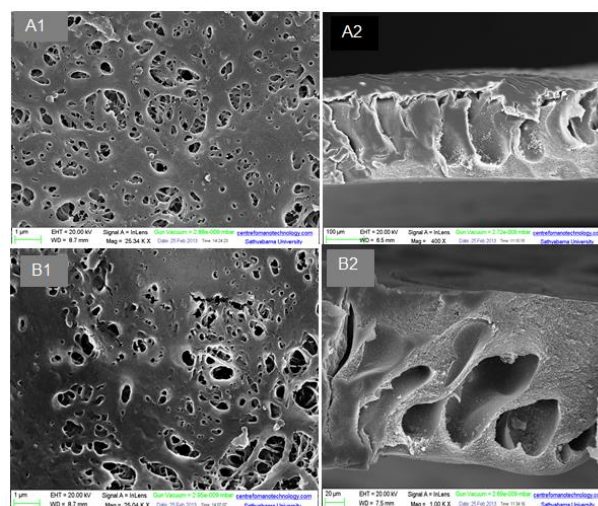


**Figure 3** SEM micrographs of top and cross-section of CA/IO (A1 and A2) and CA/AC (B1 and B2) MMMs

### 3.3 Pure Water Flux Studies

The water flux studies were performed for all synthesized membranes and the steady state flux values were reported as shown in Figure 4. The highest flux of 11.22 Lm<sup>-2</sup>h<sup>-1</sup> was offered by CA/AC3 membrane which suggests that the increase in AC content increases. The addition of AC into the polymeric matrix will change its chemical properties, pore size distribution, porosity, and hence the filtration flux increased [20]. The skin-layer thickness and sub-layer porosity as well as the surface pores size of CA/AC MMMs intensively altered the permeate flux. Similarly, IO nanoparticles with minimal loading of 0.5 wt % also influenced the permeability to 7.17 Lm<sup>-2</sup>h<sup>-1</sup> due to its hydrophilicity offering (O) radicals. However, higher loadings of 1.5 and 2.5 wt % lead to decreased flux lesser than the flux rate of neat CA. Hence, for effluent treatment CA with

highest AC (CA/AC3) and lowest IO loading (CA/IO) has been chosen and investigated.

### 3.4 Efficiency of Polymer Assisted UF

The polymer enhanced UF conjugated with synthesized CA virgin membrane resulted in permeate flux of  $2.56 \text{ Lm}^{-2}\text{h}^{-1}$  which is 48.43 % lower compared to effluent treated without PEI complexation. The flux obtained on treatment with synthesized MMMs showed flux of  $4.135 \text{ Lm}^{-2}\text{h}^{-1}$  for IO containing MMM and  $3.245 \text{ Lm}^{-2}\text{h}^{-1}$  for AC containing MMM due to PEI binding. Figure 5 shows the effect of PEI on flux decrease and the comparison of it with flux of effluent having no PEI and also pure water flux. The rejection ability of CA and each adsorbent based MMM were evaluated by the concentration of COD, BOD and sulphates contained in permeate and reject after each run using effluent with and without polymer binding.

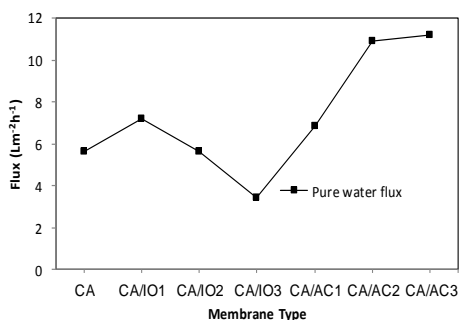


Figure 4 Pure water flux studies on synthesized MMMs

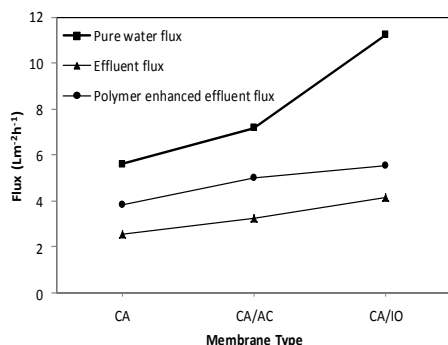


Figure 5 Effect of PEI on flux of textile dye effluent

#### 3.4.1 Effect of PEI Complexation on BOD Removal

The BOD removal is highly intense for CA/IO MMM operated with PEI bound effluent that showed about 96.7% reduction as owing to fouling resistant ability of magnetite nanoparticles. The reject BOD concentration is 84 mg/l that ensures the adsorption capacity of IO impregnated in CA matrix. However, the reject volume of neat CA and CA/AC MMMs as shown in Figure 6 indicated increase in concentration of BOD of about 372 and 284 respectively. It can be concluded that superior hydrophilicity of CA/IO would also be the reason for reducing the irreversible fouling and resulted in higher flux with lesser % rejection.

#### 3.4.2 Effect of PEI Complexation on COD Removal

Similar to BOD, the rejection efficiency of CA/IO in reducing COD was higher of about 89.86 % with the reject concentration of 654 mg/l, as shown in Figure 7. The natural organic matter (NOM) and heavy metal concentration were greatly reduced and there had been evidences in using iron nanoparticles coated membranes for such removal [21-23]. Like IO nanoparticles, the presence of AC in CA/AC MMM has also influenced the COD rejection efficiency to about 89.2% owing to the addition of PEI. However, the reject COD concentration was high of about 944 mg/l as compared to 654 mg/l, which was the COD reject concentrate due to CA/IO MMMs.

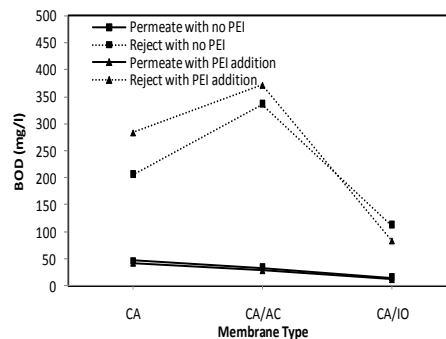


Figure 6 Effect of PEI and IO nanoparticles on BOD removal

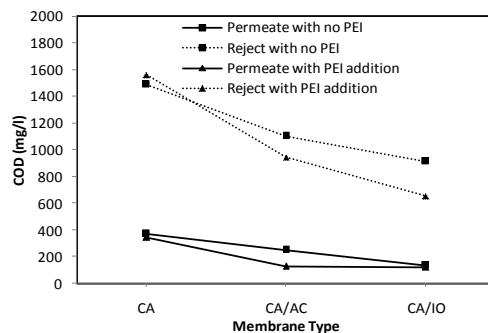


Figure 7 Effect of PEI and IO nanoparticles on COD removal

#### 3.4.3 Effect of PEI Complexation on Sulphate Removal

In contrast to BOD and COD rejection efficiency, the highest sulphates rejection was observed to be 65.8% for PEI complexed effluent treated using CA/IO MMM (Figure 8). The reason for lesser rejection is attributed to the fact that the dissolved salts pass through pores of UF membranes easily resulting in only less % rejection in comparison with that of COD and BOD. The CA/AC MMMs showed 44.72% sulphate rejection better than neat CA as it was observed to have only 12.8% sulphate rejection. These results confirm that the reducing ability of AC and IO nanoparticles present in CA matrix.

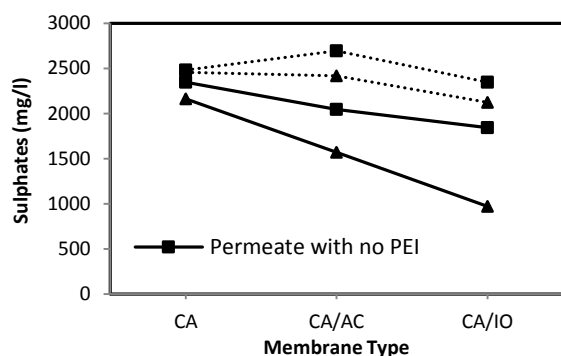


Figure 8 Effect of PEI and IO nanoparticles on sulphate removal

#### 4.0 CONCLUSION

The greener method of magnetite nanoparticles synthesis was carried out in this study and compared with the AC for its adsorption and rejection efficiency. The effect of nanoparticles loading in CA matrix was widely investigated based on the permeability flux and pore morphology. The pore size distribution and crystallite size owing to the addition of adsorbents was studied using XRD and FESEM characterization. The advantage of adsorption in decreasing the concentration of COD, BOD and sulphates in the textile effluent reject was the major breakthrough in this polymer enhanced UF study.

#### References

- [1] Walther, H. J., Faust, S. D., Aly, O. M. 1988. *Acta Hydroch. Hydrob.* 16: 572.
- [2] Choy, K. K. H., McKay, G., Porter, J. F. 1999. Sorption of Acid Dyes from Effluents Using Activated Carbon. *Resour. Conserv. Recy.* 27 (1–2): 57–71.
- [3] Kannan, N., Sundaram, M.M. 2001. Kinetics and Mechanism of Removal of Methylene Blue by Adsorption on Various Carbons- A Comparative Study. *Dyes Pigm.* 51(1): 25–40.
- [4] Namasivayam, C., Kavitha, D. 2002. Removal of Congo Red from Water by Adsorption onto Activated Carbon Prepared from Coir Pith, An Agricultural Solid Waste. *Dyes Pigm.* 54: 47–58.
- [5] Malik, P.K. 2003. Use of Activated Carbons Prepared from Sawdust and Rice-husk for Adsorption of Acid Dyes: A Case Study of Acid Yellow 36. *Dyes Pigm.* 56(3): 239–249.
- [6] Marsh, H., Rodríguez-Reinoso, F. 2006. *Activated Carbon*. First ed. Elsevier, Oxford.
- [7] Ballinas, L., Torras, C., Fierro, V., Garcia-Valls, R. 2004. Factors Influencing Activated Carbon-polymeric Composite Membrane Structure and Performance. *J. Phys. Chem. Solids.* 65(2–3): 633–637.
- [8] Kusworo, T. D., Ismail, A. F., Mustafa, A., Budiyo. 2010. The Effect of Functionalization Carbon Nanotubes (Cnts) on the Performance of PES-CNTs Mixed Matrix Membrane. *Internat. J. of Sci. and Eng.* 1(1):15–20.
- [9] Zhang, W. X. 2003. Nanoscale Iron Particles for Environmental Remediation: An Overview. *J. Nanopart. Res.* 5: 323–332.
- [10] Li, X. Q., Brown, D., Zhang, W. X. 2007. Stabilization of Biosolids with Nanoscale Zero-valent Iron (nZVI). *J. Nanopart. Res.* 9(2): 233–243.
- [11] Xu, J., Dozier, A., Bhattacharyya, D. 2005. Synthesis of Nanoscale Bimetallic Particles in Polyelectrolyte Membrane Matrix for Reductive Transformation of Halogenated Organic Compounds. *J. Nanopart. Res.* 7(4–5): 449–467.
- [12] Tratnyek, P. G., Johnson, R. L. 2006. Nanotechnologies for Environmental Cleanup. *Nano Today.* 1(2): 44–48.
- [13] Pignatello, J.J., Oliveros, E., MacKay, A. 2006. Advanced Oxidation Processes for Organic Contaminant Destruction Based on the Fenton Reaction and Related Chemistry. *Critical Rev. Environ. Sci. Technol.* 36: 1–84.
- [14] Laine, D.F., Cheng, I.F. 2007. The destruction of organic pollutants under mild reaction conditions: A review. *Microchem. J.* 85(2):183–193.
- [15] Martínez-Mera, I., Espinosa-Pesqueira, M. E., Pérez-Hernández, R., Arenas-Alatorre, J. 2007. Synthesis of Magnetite (Fe<sub>3</sub>O<sub>4</sub>) Nanoparticles Without Surfactants at Room Temperature. *Mater. Lett.* 61(23): 4447–4451.
- [16] Smuleac, V., Bachas, L., Bhattacharyya, D. 2010. Aqueous-phase Synthesis of PAA in PVDF Membrane Pores for Nanoparticle Synthesis and Dichlorobiphenyl Degradation. *J. Membr. Sci.* 346(2): 310–317.
- [17] Lewis, S., Lynch, A., Bachas, L., Hampson, S., Ormsbee, L., Bhattacharyya, D. 2009. Chelate-Modified Fenton Reaction for the Degradation of Trichloroethylene in Aqueous and Two-phase Systems. *Environ. Eng. Sci.* 26(4): 849–859.
- [18] Smuleac, V., Varma, R., Sikdar, S., Bhattacharyya, D. 2011. Green Synthesis of Fe and Fe/Pd Bimetallic Nanoparticles in Membranes for Degradation of Chlorinated Organics from Water. *J. Membr. Sci.* 379(1–2): 131–137.
- [19] Prema, P., Selvarani, M. 2012. Use of Zerovalent Iron Nanoparticles as Low Cost Adsorbent in the Removal of Hexavalent Chromium from Aqueous Solution: Equilibrium and Kinetics Study. *Int. J. Res. Chem. Environ.* 2(4): 115–124.
- [20] Li, H. L., Jyh, C. C., Ming, W. Y. 2013. The Properties and Filtration Efficiency of Activated Carbon Polymer Composite Membranes for the Removal of Humic Acid. *Desalination.* 313: 166–175.
- [21] Belaiba, F., Meniai, A.H., Bencheikh-Lehocine, M., Mansri, A., Morcellet, M., Bacquet, M., Martel, B. 2004. A Macroscopic Study of the Retention Capacity of Copper B Polyaniline Coated Onto Silica Gel and Natural Solid Materials. *Desalination.* 166: 371–377.
- [22] Ng, L. Y., Mohammad, A. W., Leo, C. P., Hilal, N. 2013. *Desalination.* 308: 15–33.
- [23] Hosseini, S.M., Madaeni, S.S., Heidari, A.R., Amirimehr, A. 2012. Preparation and Characterization of Ion-selective Polyvinyl Chloride Based Heterogeneous Cation Exchange Membrane Modified by Magnetic Iron-nickel Oxide Nanoparticles. *Desalination.* 284: 191–199.